European Polymer Journal 93 (2017) 1–7

Contents lists available at ScienceDirect

European Polymer Journal

journal homepage: www.elsevier.com/locate/europolj

Customizing thermally-reduced graphene oxides for electrically conductive or mechanical reinforced epoxy nanocomposites

J.M. Vazquez-Moreno[a], V. Yuste-Sanchez[a], R. Sanchez-Hidalgo[a,b], R. Verdejo[a], M.A. Lopez-Manchado[a,*], L. Fernández-García[b], C. Blanco[b], R. Menéndez[b]

[a] Instituto de Ciencia y Tecnología de Polímeros, ICTP-CSIC, C/Juan de la Cierva 3, 28006 Madrid, Spain
[b] Instituto Nacional del Carbon, INCAR-CSIC, Apartado 73, 33080 Oviedo, Spain

ARTICLE INFO

Keywords:
Graphene
Epoxy
Brodie
Hummers
Polymer nanocomposites

ABSTRACT

Graphene oxide (GO) can be produced through diverse synthetic routes in large quantities that lead to clear differences in the resulting graphene morphology and properties. Here, we analysed the effect of several thermally reduced graphene oxides (TRGOs), at two different concentrations, on the electrical and mechanical properties of epoxy resin nanocomposites. Natural graphite was oxidised using two methods, Brodie (GO-B) and Hummers (GO-H), and, then, thermally reduced at different temperatures, 700, 1000, and 2000 °C. Intrinsic graphene properties, such as remaining oxygen groups, specific surface area, and aspect ratio, among others, have a profound effect on the final properties of the nanocomposite. The dispersion state was heavily influenced by the specific surface area and the remaining oxygen groups on the graphene. Meanwhile, the electrical and mechanical properties showed a strong and opposite dependency with the reduction temperature, with low temperatures resulting in flakes with high reinforcing characteristics and high temperatures in flakes with high electrical conductivity performance. Finally, TRGOs synthesised via Hummers and reduced at low temperatures appeared to be more suited as reinforcing particles, while TRGOs synthesised via Brodie were more effective as electrically conductive nanofillers.

1. Introduction

Over the recent years, graphene and its derivatives have emerged as a promising material on a number of applications, such as energy technologies, biomedical, liquid separation, electronic [1,2]. Among these materials, graphene oxide (GO) and reduced graphene oxide are being heavily studied as reinforcing and functional nanofillers in polymer materials [3–7] due to their excellent physical and chemical properties and their potential to be produced on the ton scale. Common synthesis routes are the Hummers, Staudenmaier and Brodie methods, which have been suggested to result in differences in the levels of oxidation and final structure of the GO [1,2]. Such differences could significantly affect the final properties of the resulting polymer nanocomposite and could pave the way for the production of tailor-made graphene materials. Here, we investigate such hypothesis by analysing the effect of distinct thermally reduced graphene oxide (TRGO) on the performance of an epoxy resin with special attention to its mechanical and electrical properties.

In a previous work [8], we demonstrate that both the oxidation process of the graphite and the exfoliation temperature of the oxide play a crucial role on the characteristics of the resultant graphene. We thoroughly analysed the resulting material of two

* Corresponding author.
E-mail address: lmanchado@ictp.csic.es (M.A. Lopez-Manchado).

http://dx.doi.org/10.1016/j.eurpolymj.2017.05.026
Received 22 March 2017; Received in revised form 9 May 2017; Accepted 16 May 2017
Available online 18 May 2017
0014-3057/ © 2017 Elsevier Ltd. All rights reserved.

oxidising protocols, Brodie and Hummers, and established crucial differences among them. Brodie method introduces a smaller amount of oxygen than Hummers, but favours the formation of conjugated epoxy groups and hydroxyl, that at moderate temperatures generates groups that are more thermally stable. Thus, the Csp^2 structure of the carbon lattice is not recovered at all, and some of the residual oxygen cannot be removed. However, GO obtained through Hummers oxidation method exhibits less conjugated oxygen groups resulting in a better restoration of the sp^2 structure. In addition, the functional groups content is clearly decreased as increasing the exfoliation temperature of the graphite oxide. So, GO obtained by the Hummers process contains 47.8% of oxygen, whereas that reduced at 700 °C exhibits an 11.1% and at 2000 °C, the oxygen content is practically negligible.

Epoxy resins are an important class of polymers due to their strong adhesion and excellent overall mechanical properties, high chemical, thermal, and dimensional stability and solvent resistance. The intrinsic properties of epoxy resins make them suitable for a wide spectrum of applications in diverse areas due to the fact that epoxies can be chemically and physically tailored to fulfil specific requirements. Several interesting studies have already been reported illustrating the potential of graphene nanocomposites based on epoxy resin [9–18]. These studies have shown large improvements on the mechanical and electrical properties of the epoxy nanocomposites. Graphene/epoxy nanocomposites have thoroughly been reviewed by Wei et al. [19].

The aim of this paper is to analyse the effect of the structure and morphology of the graphene on the physical and mechanical properties of the resin composite, which to the authors' best knowledge has not previously been studied.

2. Experimental section

2.1. Materials

Hexflow RTM 6 monocomponent epoxy system used in this study was gently provided by Hexcel. Thermal reduced graphite oxide (TRGO) was obtained by the rapid thermal expansion of graphite oxide (GO) at several temperatures: 700, 1000 and 2000 °C. GO was previously synthesised from natural graphite powder, purchased from Sigma-Aldrich (universal grade, purum powder 60.1 mm, 200 mesh, 99.9995%), following two oxidation protocols, Brodie and modified Hummers methods. The main characteristics of the studied materials are detailed in Table 1. The samples are labelled as TRGH-700, TRGH-1000, TRGH-2000, TRGB-700, TRGB-1000 and TRGB-2000, where H and B refer to the oxidation method (H: Hummers and B: Brodie).

2.2. Preparation of TRGOs/epoxy nanocomposites

The dispersion of the TRGOs in the epoxy resin was carried out by means of a three-roll calender (EXAKT 80E), where contra-rotating rollers exert large shear forces in the knead-vortex generated between them. The materials were prepared at two TRGO contents: 1.5 and 2 wt.%. The optimal processing conditions were previously evaluated and the procedure used to achieve a fine dispersion of the flakes in the epoxy resin consists of three cycles. Details of the processing parameters, time, roller gap and velocity are presented in Table 2.

Once the mixing process has been completed, the blends were degassed for 1 h at room temperature in a vacuum chamber. Subsequently, the material was poured into preheated silicone moulds for its mechanical and electrical characterisation. The samples were cured in an oven at 160 °C for 2 h and then, post-cured at 180 °C for 1 h.

2.3. Characterisation

Optical microscopy images were taken with a NIKON DS–Fi2 microscope in order to evaluate the dispersion degree of TRGOs in the liquid formulations. The curing process was examined in a Mettler Toledo DSC822 differential scanning calorimetry. The samples were held at an isothermal scan of 160 °C. The morphology of the cured samples was observed using a Philips XL30 environmental scanning electron microscopy (ESEM) at 15 kV. The fractured cross-sections from tensile tests were sputter coated with gold/palladium (Au/Pd 80/20) in order to prevent electrical discharge during observation.

Tensile tests were measured according to ASTM D 3379-75 specifications in an Instron dynamometer (model 3366) at 23 °C, and

Table 1
Main characteristics of GOs and TRGOs.

	Elemental analysis (wt.%)			XPS					S_{BET} m^2/g
	C	O	H	C/O	O (%)	C (%)	sp^2 (%)	sp^3 (%)	
GO-H	48.0	47.8	2.2	1.8	35.2	64.8	32.2	12.8	–
TRGH-700	87.8	11.1	0.8	9.2	9.8	90.2	74.6	15.1	390
TRGH-1000	97.9	1.1	0.1	57.8	1.7	98.3	82.4	13.9	300
TRGH-2000	99.5	0.5	0.0	332.3	0.3	99.7	88.9	9.6	140
GO-B	70.1	28.2	0.9	2.9	25.7	74.3	39.2	14.5	–
TRGB-700	90.1	9.7	0.2	13.1	7.1	92.9	75.0	13.1	660
TRGB-1000	98.0	1.6	0.3	25.3	3.8	96.2	77.3	14.1	570
TRGB-2000	99.3	0.7	0.0	37.5	2.6	97.4	81.8	13.0	140

Table 2
Calender process parameters.

	Gap 1, μm	Gap 2, μm	Velocity, rpm	Time, min
Cycle 1	100	50	350	10
Cycle 2	50	25	350	10
Cycle 3	25	5	350	25

at a cross-head speed of 5 mm/min. At least five specimens of each sample were tested to determine a mean value of the results.

Electrical conductivity of the cured nanocomposites was determined on an ALPHA high resolution dielectric analyser (Novocontrol Technologies GmbH) over a frequency range window of 10^{-1}–10^{7} Hz at room temperature. The cured films were held in the dielectric cell between two parallel gold-plated electrodes. The amplitude of the alternating current electric signal applied to the samples was 1 V.

3. Results and discussion

3.1. Morphology

The degree of dispersion of the TRGO in the liquid epoxy resin prior to its curing is investigated by optical microscopy. The images in Fig. 1 show that, in general, all TRGOs are homogeneously dispersed in the epoxy, indicating that the three-roll milling is an effective method to disperse the flakes in the liquid resin. The TRGOs thermally reduced al lower temperatures, 700 °C show a more homogeneous dispersion in the resin and a lower agglomerate size due both to the presence of a higher content of functional groups on its structure and its larger surface area. Furthermore, TRGOs synthesised by Brodie exhibit less agglomerates as compared to Hummers TRGOs. The different dispersion state could be attributed to the observed differences on the BET surface area between the Hummers and Brodie methods, being the later almost twice the BET surface area of the former. The larger surface area of the Brodie method should facilitate the intercalation of the polymer chain within the layers and the breakage of the agglomerates.

These results were corroborated by the SEM images of the cured samples (Fig. 2) where no large agglomerates were observed. This observation indicates that the graphene dispersion is not altered during the curing. As indicated, TRGB-700 and TRGH-700 show a finer and more homogeneous dispersion in the resin matrix. In addition, it is observed that the fracture surface of the pristine epoxy resin is smooth showing regular river patterns. Thus, the fracture pattern of net epoxy resin exhibits a brittle fracture. Meanwhile, the addition of TRGOs changes the fracture surface of the composites, becoming rougher with the appearance of cracks on it. Similar results have previously been reported on similar TRGOs/epoxy nanocomposites and suggested a correlation between surface roughness and fracture toughness [12,20,21]. The high level of roughness observed on the fracture surfaces of these systems has been related to the flake thickness and the good filler/matrix interaction due to the presence of remaining oxide groups [20,21]. Additionally, the two main toughening mechanisms of graphene based epoxy composites have been ascribed to crack pinning by the nanofiller and separation between the graphitic layers [20]. Finally, TRGH-700 appears to present higher roughness level than TRGB-700, which suggests a higher toughening ability (discussed below).

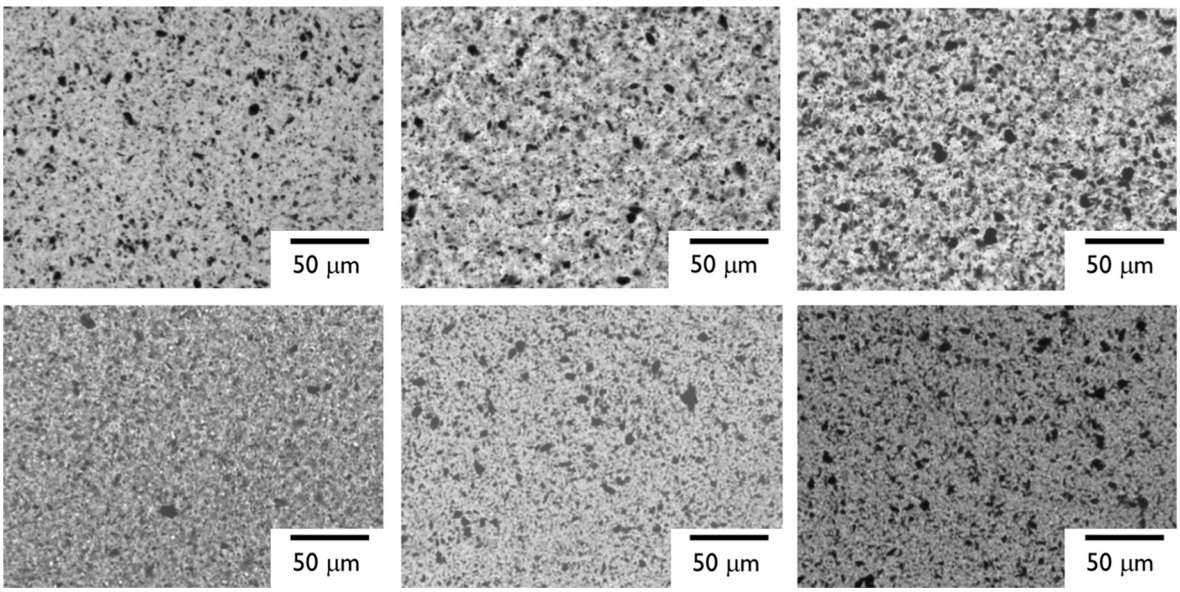

Fig. 1. Epoxy dispersions with 2 wt.% TRGO. From top to bottom and left to right: TRGH-700, TRGH-1000, TRGH-2000, TRGB-700, TRGB-1000 and TRGB-2000.

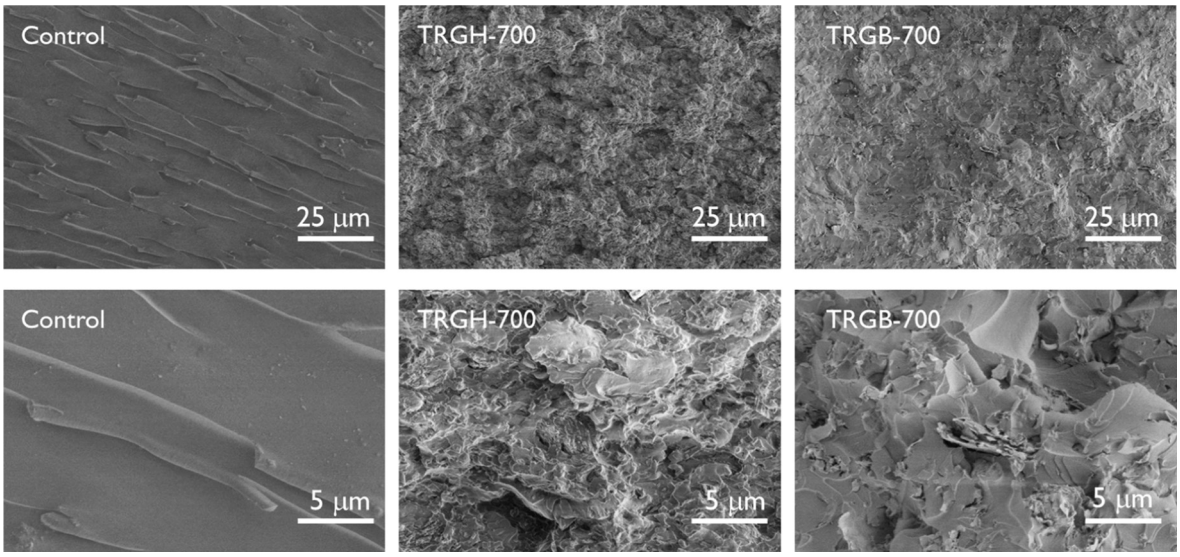

Fig. 2. Representative SEM images of the TRGOs/epoxy resin nanocomposites showing the effect of the oxidation method in the dispersion.

Isothermal DSC scans at 160 °C were used to determine the effect of the TRGOs on the evolution of the epoxy resins during the curing process. The addition of TRGOs causes an acceleration of the curing reaction showing a clear trend with the exfoliation temperature: the lower the exfoliation temperature, the faster the cure reaction proceeds (Fig. 3). This catalytic behaviour of the nanoparticles is attributed to the presence of functional groups, mainly carbonyl, hydroxyl and epoxy, on the graphene structure. Low temperature reduced TRGOs, 700 °C, presented a higher number of functional groups on its structure, than those reduced at 2000 °C which presents a similar rate to the epoxy resin. Furthermore, no significant differences are observed between both oxidation methods. Previous studies with both carbon nanotubes [22] and graphene oxides [11] have also reported a similar catalytic behaviour in epoxy resins.

3.2. Mechanical properties

The tensile response at room temperature of the nanocomposites is shown in Table 3. RTM 6 epoxy resin is a brittle and tough material with high Young's modulus, extraordinary tensile strength and relatively low elongation at break.

Although the materials obtained by both oxidation methods appear to have a similar trend, with the low temperature TRGOs showing higher reinforcing effect, there are clear differences among Hummers and Brodie TRGOs. Hummers TRGOs present a strong dependency of their reinforcing character with the exfoliation temperature, while the reinforcing character of Brodie TRGOs is less dependent with it (Fig. 4). Such effect is consistent with the different stability of the functional groups with the temperature of the two oxidation protocols. As shown in Table 1, although GO-H has a higher amount of oxygen functional groups (C/O of 1.8 in GO-H vs 2.9 in GO-B), their elimination at moderate temperatures is more pronounced, which would then limit the formation of filler/matrix interactions and result in the dramatic decrease of the mechanical properties of the composite.

Overall TRGH-700 is the most effective nanofiller to improve the mechanical properties of the resin nanocomposites showing an

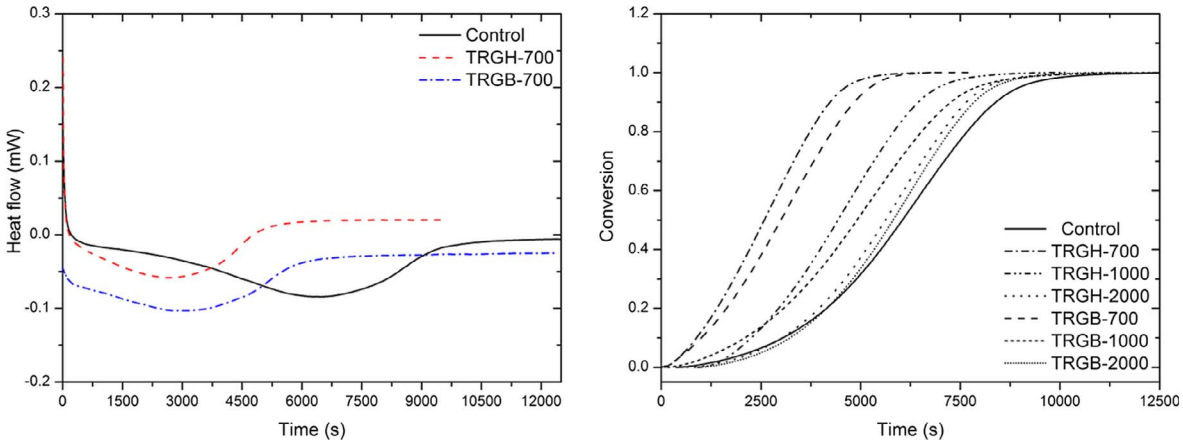

Fig. 3. DSC isothermal curves showing the effect of the oxidation protocol and conversion.

Table 3
Mechanical properties of TRGOs/epoxy resin nanocomposites.

Sample	Young's modulus, MPa	Strength max., MPa	Elongation at break, %
RTM 6	2110 ± 44	61 ± 5	6.1 ± 0.8
TRGH-700 1.5%	2248 ± 46	56 ± 4	5.5 ± 0.7
TRGH-700 2%	2457 ± 51	51 ± 3	4.6 ± 0.6
TRGH-1000 1.5%	1958 ± 34	49 ± 5	3.6 ± 0.7
TRGH-1000 2%	2102 ± 42	48 ± 5	3.6 ± 0.5
TRGH-2000 1.5%	1782 ± 32	44 ± 4	3.5 ± 0.7
TRGH-2000 2%	1835 ± 34	42 ± 3	3.4 ± 0.5
TRGB-700 1.5%	2199 ± 42	55 ± 5	5.4 ± 0.7
TRGB-700 2%	2279 ± 45	53 ± 3	5.4 ± 0.4
TRGB-1000 1.5%	2071 ± 35	52 ± 3	4.9 ± 0.5
TRGB-1000 2%	2326 ± 58	50 ± 4	4.5 ± 0.6
TRGB-2000 1.5%	2048 ± 42	48 ± 3	4.4 ± 0.5
TRGB-2000 2%	2025 ± 34	44 ± 3	4.1 ± 0.4

improvement of 16% in the Young's modulus with 2 wt.% loading fraction. This result can be ascribed to two contributions, the amount of functional groups present on the surface of the graphene layers and their size. Low temperature Hummers present a higher amount of residual oxygen groups than Brodie (Table 1), and, hence, they should form a stronger interaction with the epoxy resin. Both theoretical and experimental studies have found a direct correlation between the flake lateral sizes and the reinforcing efficiency of graphene in polymer nanocomposites [23–26], which has been ascribed to an enhanced filler-to-matrix contact area. We have previously reported that the lateral size of the Brodie layers were smaller than the Hummers layers [8], consistent with those previous studies.

The elongation at break of the nanocomposite decreases by the addition of TRGO. No significant differences with the oxidation method and the exfoliation temperature are observed. This reduction of the elongation at break is commonly observed on epoxy nanocomposites reinforced with carbon-based epoxy [14].

3.3. Electrical conductivity

The AC electrical conductivity at room temperature as a function of frequency is shown in Fig. 5. The electrical conductivities of all samples with 1.5 wt.% TRGO show a linear dependency with the frequency, characteristic of dielectric materials (Fig. S1). Hence, the electrical percolation is attained above 1.5 wt.% loading fraction, independently of the type of TRGOs used. Such high percolation threshold could be related to the flexibility of these nanofillers, which is a direct consequence of their wrinkled morphology [27,28]. Recent theoretical investigations have shown that flexible nanofillers are less likely to form a percolating network as they become less anisotropic [28]. Once the percolation is reached, the achieved electrical conductivity shows a clear dependency with both the exfoliation temperature and oxidation protocol. It is observed that the TRGOs reduced at the highest temperature, 2000 °C, form the

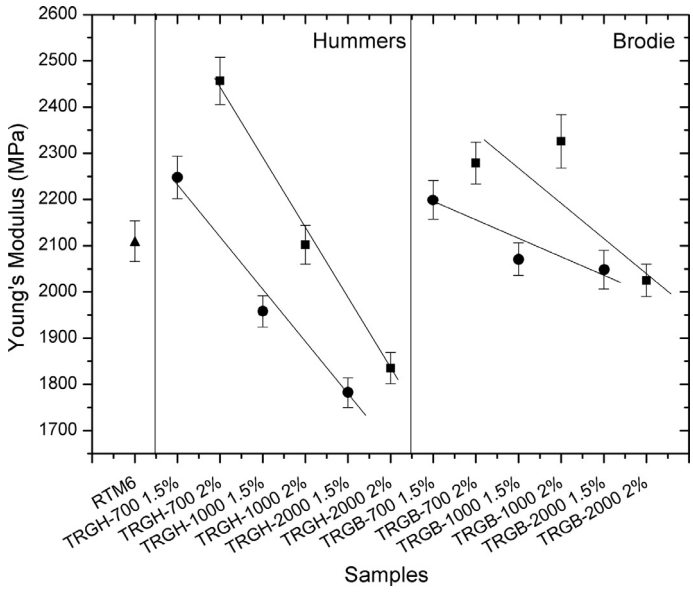

Fig. 4. Young's modulus as a function of TRGOs. Samples with 1.5 wt.% and 2 wt.% loading fraction are represented as dots and squares, respectively. The straight lines are drawn as a guide to the eyes.

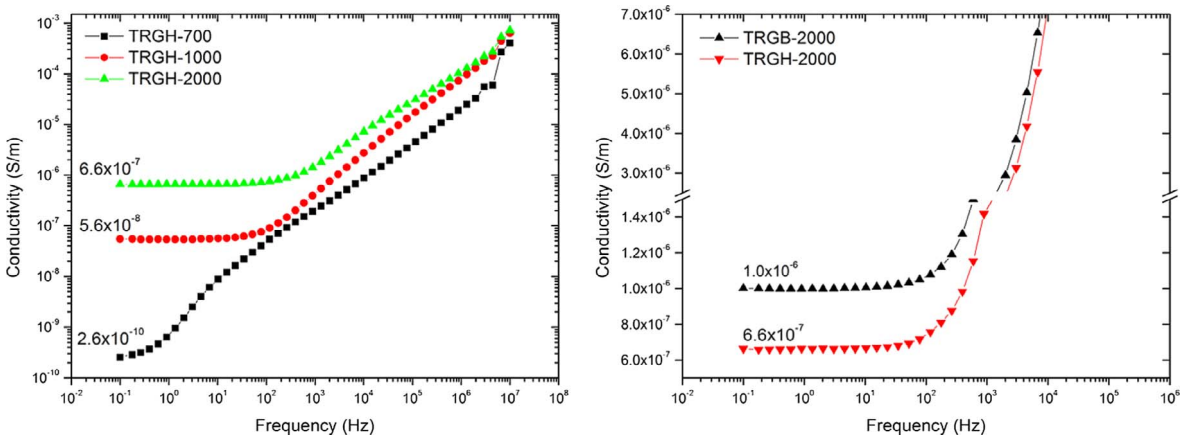

Fig. 5. Electrical conductivity of 2 wt.% TRGOs/epoxy resin nanocomposites: (left) effect of the exfoliation temperature of GO and (right) effect of the oxidation method.

most effective filler network with higher values of the electrical conductivity (Fig. 5a) reaching 1×10^{-6} S/m with TRGB-2000. This dependency of the electrical conductivity with the exfoliation temperature is the result of two combined effects: the reduction temperature efficiency, higher temperatures are able to reduce further the oxygen groups present on the surface, and the restoration of the crystalline graphitic structure as the temperature increases. Hence, it would be expected that the ideal nanofiller would have none or almost none functional groups, a restored crystalline graphitic morphology and a high aspect ratio (since several theoretical [29] and experimental results [30] have suggested that high aspect ratio particles result in a higher conductivity). However, the results show that TRGB-2000 with a smaller flake size than TRGH-2000 forms a more effective electrical network (Fig. 5b). Such result could be attributed to the already mentioned better dispersion achieved with this nanofiller, which facilitates the conduction via tunnelling between adjacent and isolated graphene layers [31].

4. Conclusions

By controlling the structure and morphology of graphene it is possible to obtain composite materials with tailored properties. It has been observed that not only the oxidation method but also the reduction temperature are key factors affecting the physical properties of the epoxy nanocomposites. Intrinsic graphene properties, such as remaining oxygen groups, specific surface area, and aspect ratio among others have a profound effect on the macroscopic properties. Thus, the material with better mechanical performance is obtained by using TRGOs reduced at low temperatures and oxidised by the Hummers method. While, to achieve a material with a high electrical conductive, it is necessary to exfoliate the graphite oxide at high temperatures, 2000 °C, and use Brodie's oxidising protocol.

Acknowledgements

The authors gratefully acknowledge the financial support of the State Secretariat for Research, Development and Innovation of the Spanish Ministry of Economía y Competitividad, through the project MAT2013-48107-C3.

Appendix A. Supplementary material

Supplementary data associated with this article can be found, in the online version, at http://dx.doi.org/10.1016/j.eurpolymj.2017.05.026.

References

[1] D. Dreyer, S. Park, C. Bielawski, R. Ruoff, Harnessing the chemistry of graphene oxide, Chem. Soc. Rev. 43 (2014) 5288–5301.
[2] S. Park, R.S. Ruoff, Synthesis and characterization of chemically modified graphenes, Curr. Opin. Colloid Interface Sci. 20 (2015) 322–328.
[3] H. Kim, A.A. Abdala, C.W. Macosko, Graphene/polymer nanocomposites, Macromolecules 43 (2010) 6515–6530.
[4] T. Kuilla, S. Bhadra, D. Yao, N.H. Kim, S. Bose, J.H. Lee, Recent advances in graphene based polymer composites, Prog. Polym. Sci. 35 (2010) 1350–1375.
[5] R. Verdejo, M.M. Bernal, L.J. Romasanta, M. Lopez-Manchado, Graphene filled polymer nanocomposites, J. Mater. Chem. 21 (2011) 3301–3310.
[6] J.J. Phiri, P. Gane, T.C. Maloney, General overview of graphene: production, properties and application in polymer composites, Mater. Sci. Eng., B 215 (2017) 9–28.
[7] M. Zhang, Y. Li, Z. Su, G. Wei, Recent advances in the synthesis and applications of graphene–polymer nanocomposites, Polym. Chem. 6 (2015) 6107–6124.
[8] C. Botas, P. Álvarez, P. Blanco, M. Granda, C. Blanco, R. Santamaría, et al., Graphene materials with different structures prepared from the same graphite by the Hummers and Brodie methods, Carbon 65 (2013) 156–164.
[9] M.A. Rafiee, J. Rafiee, Z. Wang, H. Song, Z.-Z. Yu, N. Koratkar, Enhanced mechanical properties of nanocomposites at low graphene content, ACS Nano 3 (2009) 3884–3890.
[10] M.A. Rafiee, J. Rafiee, I. Srivastava, Z. Wang, H. Song, Z.-Z. Yu, et al., Fracture and fatigue in graphene nanocomposites, Small 6 (2010) 179–183.

[11] S.L. Qiu, C.S. Wang, Y.T. Wang, C.G. Liu, X.Y. Chen, H.F. Xie, et al., Effects of graphene oxides on the cure behaviors of a tetrafunctional epoxy resin, Expr. Polym. Lett. 5 (2011) 809–818.
[12] M. Martin-Gallego, R. Verdejo, M.A. Lopez-Manchado, M. Sangermano, Epoxy-graphene UV-cured nanocomposites, Polymer 52 (2011) 4664–4669.
[13] W.K. Li, A. Dichiara, J.B. Bai, Carbon nanotubes-graphene nanoplatelet hybrids as high performance multifunctional reinforcements in epoxy composites, Compos. Sci. Technol. 74 (2013) 221–227.
[14] M. Martin-Gallego, M.M. Bernal, M. Hernandez, R. Verdejo, M.A. Lopez-Manchado, Comparison of filler percolation and mechanical properties in graphene and carbon nanotubes filled epoxy nanocomposites, Eur. Polym. J. 49 (2013) 1347–1353.
[15] S.G. Prolongo, A. Jimenez-Suarez, R. Moriche, A. Ureña, In situ processing of epoxy composites reinforced with graphene nanoplatelets, Compos. Sci. Technol. 86 (2013) 185–191.
[16] S.G. Prolongo, A. Jimenez-Suarez, R. Moriche, A. Ureña, Graphene nanoplatelets thickness and lateral size influence on the morphology and behavior of epoxy composites, Eur. Polym. J. 53 (2014) 292–301.
[17] R. Moriche, S.G. Prolongo, M. Sanchez, A. Jimenez-Suarez, M.J. Sayagua, A. Ureña, Morphological changes on graphene nanoplatelets induced during dispersion into an epoxy resin by different methods, Compos. Part B-Eng. 72 (2015) 199–205.
[18] J.E. An, Y.G. Jeong, Structure and electric heating performance of graphene/epoxy composite films, Eur. Polym. J. 49 (2013) 1322–1330.
[19] J. Wei, T. Vo, F. Inam, Epoxy/graphene nanocomposites – processing and properties: a review, RSC Adv. 5 (2015) 3510–73524.
[20] S. Chandrasekaran, N. Sato, F. Tölle, R. Mülhaupt, B. Fiedler, K. Schulte, Fracture toughness and failure mechanism of graphene based epoxy composites, Compos. Sci. Technol. 97 (2014) 90–99.
[21] M. Quaresimin, K. Schulte, M. Zappalorto, S. Chandrasekaran, Toughening mechanisms in polymer nanocomposites: from experiments to modelling, Compos. Sci. Technol. 123 (2016) 187–204.
[22] A. Terenzi, C. Vedova, G. Lelli, J. Mijovic, L. Torre, L. Valentini, et al., Chemorheological behaviour of double-walled carbon nanotube-epoxy nanocomposites, Compos. Sci. Technol. 68 (2008) 1862–1868.
[23] U. Khan, P. May, A. O'Neill, J.N. Coleman, Development of stiff, strong, yet tough composites by the addition of solvent exfoliated graphene to polyurethane, Carbon 48 (2010) 4035–4041.
[24] L. Gong, I.A. Kinloch, R.J. Young, I. Riaz, R. Jalil, K.S. Novoselov, Interfacial stress transfer in a graphene monolayer nanocomposite, Adv. Mater. 22 (2010) 2694–2697.
[25] P. May, U. Khan, A. O'Neill, J.N. Coleman, Approaching the theoretical limit for reinforcing polymers with graphene, J. Mater. Chem. 22 (2012) 1278–1282.
[26] J. Kim, J. Kim, S. Song, S. Zhang, J. Cha, K. Kim, H. Yoon, Y. Jung, K.W. Paik, S. Jeon, Strength dependence of epoxy composites on the average filler size of non-oxidized graphene flake, Carbon 113 (2017) 379–386.
[27] Y.B. Yi, E. Tawerghi, Geometric percolation thresholds of interpenetrating plates in three-dimensional space, Phys. Rev. E Stat. Nonlin. Soft Matter Phys. 79 (2009) 041134.
[28] S. Kwon, H.W. Cho, G. Gwon, H. Kim, B.J. Sung, Effects of shape and flexibility of conductive fillers in nanocomposites on percolating network formation and electrical conductivity, Phys. Rev. E 93 (2016) art. no. 032501.
[29] R.A. Vaia, J.F. Maguire, Polymer nanocomposites with prescribed morphology: going beyond nanoparticle-filled polymers, Chem. Mater. 19 (2007) 2736–2751.
[30] P. Akcora, H. Liu, S.K. Kumar, J. Moll, Y. Li, B.C. Benicewicz, et al., Anisotropic self-assembly of spherical polymer-grafted nanoparticles, Nat. Mater. 8 (2009) 354–359.
[31] D. Toker, D. Azulay, N. Shimoni, I. Balberg, O. Millo, Tunneling and percolation in metal-insulator composite materials, Phys. Rev. B Condens. Matter Mat. Phys. 68 (2003) 414031–414034.